Chapter 4

THE SAMPLES

For the ultrasonic experiments two types of rock were chosen: Most of the experiments were performed on an amphibolite from Gebl el Asr, SW Egypt [1] [Franz, 1987], hereafter referred to as *Chephren amphibolite*. Several hand pieces were provided by professor Franz, Technical University Berlin. Additionally, one experiment was run with a serpentinite from the jurassic Malenco unit, which represents a south-penninic ophiolite [Trommsdorff & Evans, 1972]. Diverse diagnostic methods, electron microprobing in combination with X-ray diffraction and IR-spectroscopy, were applied to determine the composition, microstructure, and water content of the samples and are given in Appendix A. To investigate the changes in the samples during the experiments, samples were quenched at the end of an experiment and analysed for decomposition of minerals, precipitations, and microcracking. The knowledge of these variations forms the basis for the interpretation of the ultrasonic experiments (Chapter 6).

4.1   Chephren Amphibolite

4.1.1   Mineral Assemblage

Strictly speaking, the *Chephren amphibolite* is a foliated granulite-facies hornblende gneiss (density: 2.82 g/cm^3), consisting of 61.1 vol% plagioclase and 34.3 vol% amphibole and is, in a first approximation, a two-component system (Fig. 4.1). The plagioclases occur as euhedral crystals with a composition ranging between An_{71} and An_{88}. The amphibole is found to be rich in Ca. When plotting the $Mg/Mg + Fe^{2+}$-ratio against the Si content, two groups of amphiboles can be distinguished: primary tschermakite/ magnesio-hornblende and secondary actinolite, which accounts for 10.4 vol% of the amphibole content. In thin-section the tschermakite/ magnesio-hornblende is characterised by a green colour with a green to ochre pleochroism. Commonly, these amphiboles are euhedral to subhedral and form larger aggregates. The actinolite occurs preferentially at the margins of larger amphibole aggregates

---

[1]In the literature this rock is sometimes referred to as "Chephren Diorite", but after Franz [1987] it is a metamorphic amphibolite of sedimentary origin.
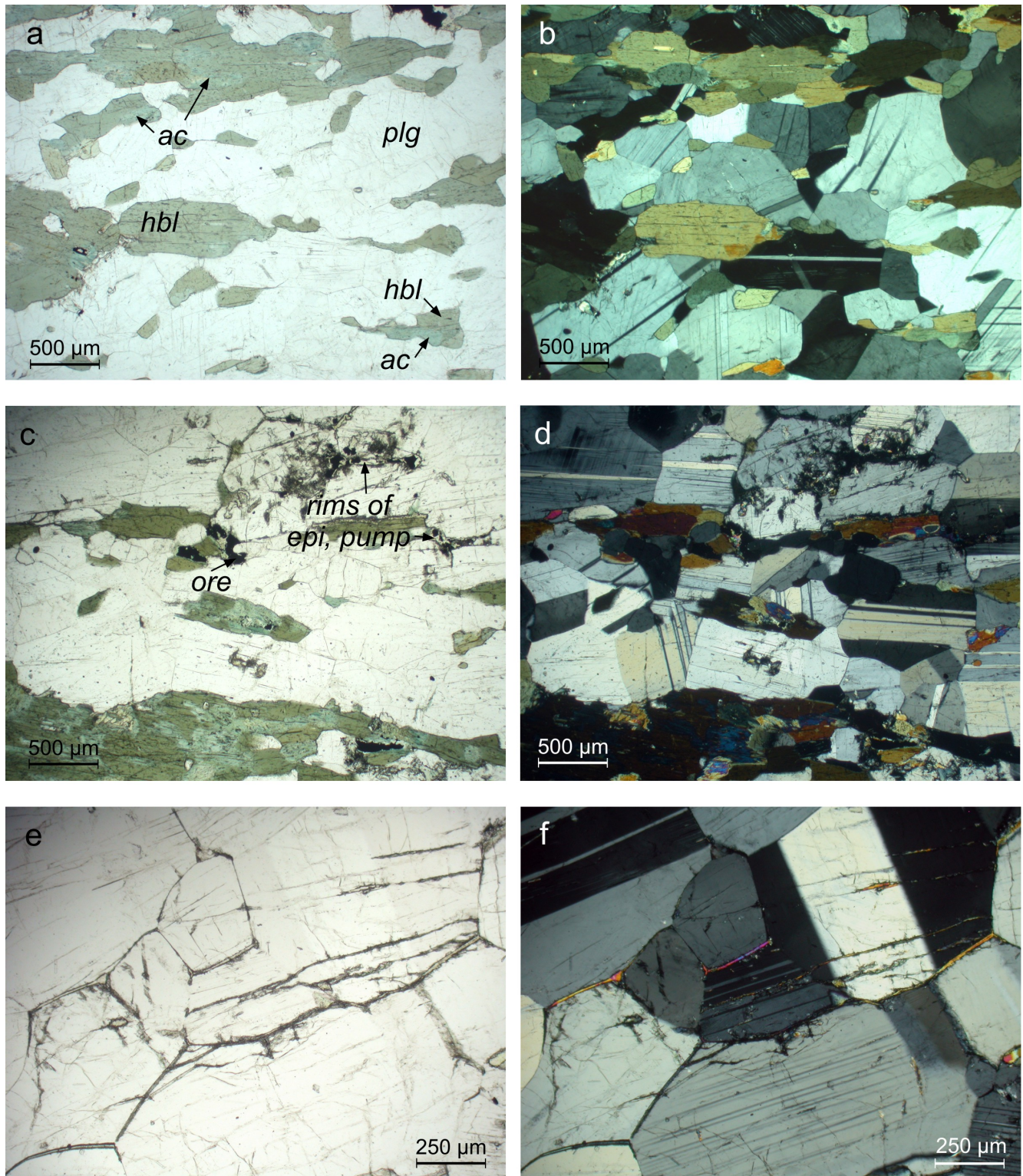
Figure 4.1: *Micrographs of Chephren amphibolite (starting material/ before PT-experiments were carried out), recorded with parallel and crossed polarisers. The mineral content is dominated by plagioclase and amphiboles. Minor minerals, such as epidote and pumpellyite form rims around ore grains (c and d) or fill grain boundaries (e and f). A slight alteration is noted near ore grains. plg: plagioclase, hbl: magnesiohornblende/ tschermakite, ac: actinolite*

.

and is characterised by light green to bluish areas in the green to dark green magnesio-hornblende. Together with the minor minerals epidote (2.6 vol%) and pumpellyite (1.2 vol%), and accessories chlorite (0.4 vol%), apatite, and muscovite the actinolite reflects a slight greenschist metamorphic overprinting of the Chephren amphibolite. Epidote, pumpellyite, and mica are not uniformly distributed throughout thin-sections. Where they are present, they fill triple junctions, grain boundaries, and cracks in plagioclase and appear along the cleavage of amphiboles (Fig. 4.1c to f). Additionally, ore grains are often surrounded by rims of epidote and pumpellyite, respectively (Fig. 4.3a). Sporadically, altered areas can be identified in the thin-section.

Samples, which were quenched after the ultrasonic experiments at pressures of 750 to 900 MPa and in a temperature range of 450 to 800 °C, show a slight increase of alteration (Figs. 4.2 and 4.3). Plagioclase is crossed by numerous thin alteration channels, filled with sericite and hematite. Partially, amphiboles possess mourning borders or show precipitation of an opaque phase along their cleavage planes.
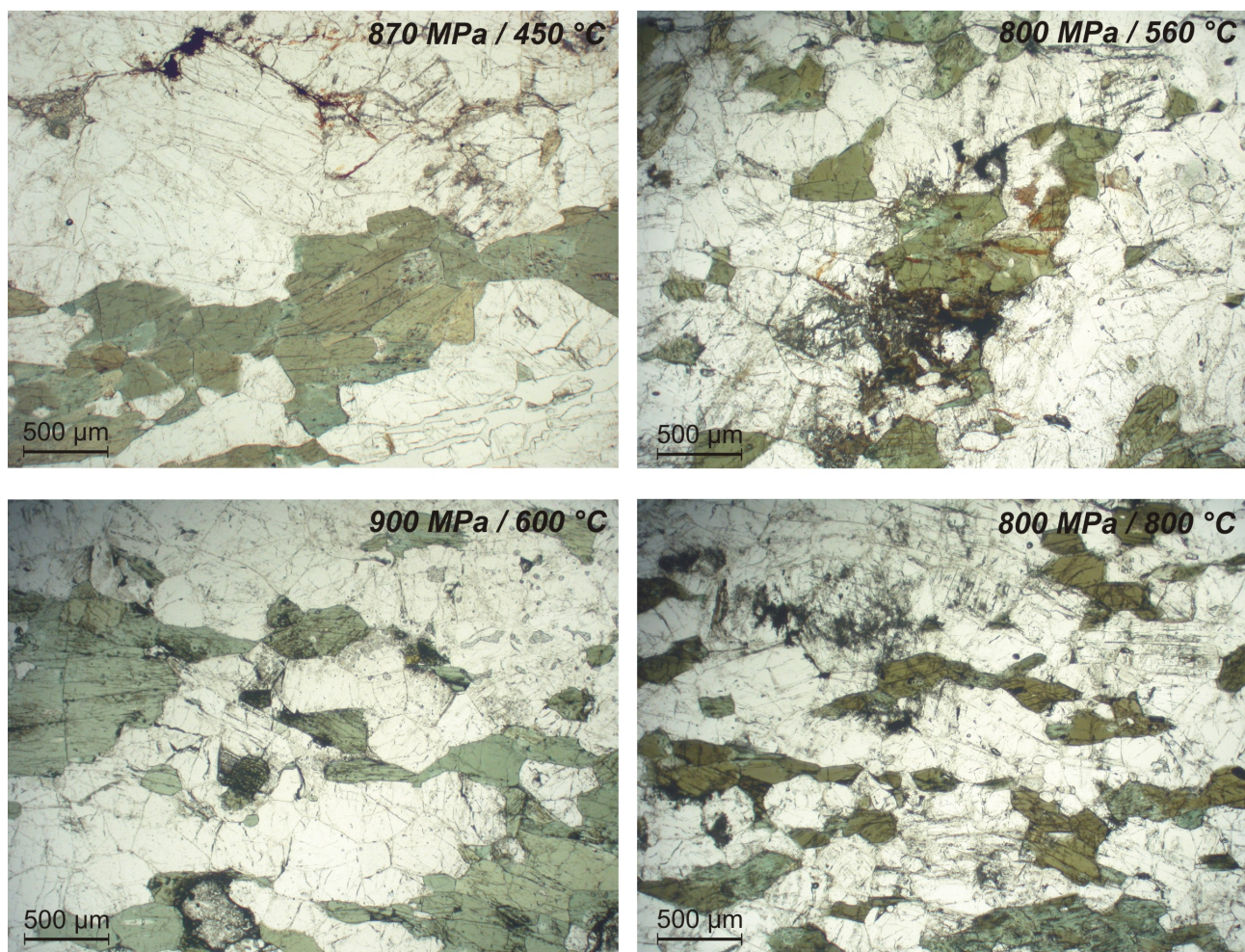

Figure 4.2: *Micrographs of quenched Chephren amphibolite, recorded with parallel polarisers. Pressure and temperature values refer to quenching conditions. Note the slight increase in alteration in comparison with the starting material (Fig. 4.1a).*
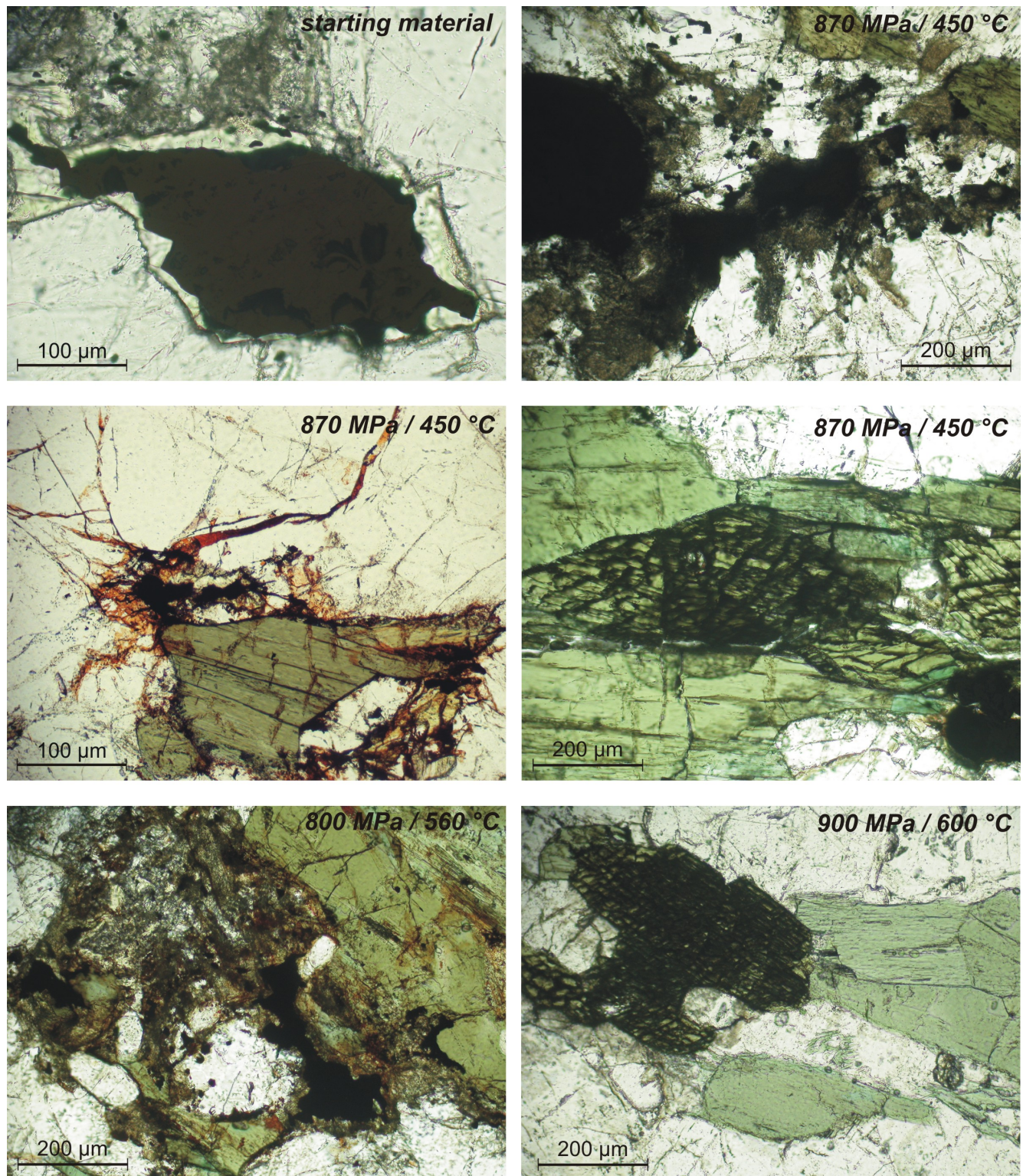
Figure 4.3: *Close-ups of original Chephren amphibolite (pre-run) (a) and quenched samples (b to f). The quenching conditions are given in the figures. (a) In the pre-run sample an ore grain is surrounded by a rim of pumpellyite with a defined extension. Above the rim an alterated zone with microcrystalline sericite and an opaque phase is observed. (b to f) The experimental conditions lead to an alteration of the rock, which can be observed especially around ore grains. Hematite (red phase in c) and opaque phases precipitate in cracks and along tthe cleavage planes of the amphiboles. Note, that alteration takes places already at 450 °C.*

The mineral reactions are usually not in thermodynamic equilibrium because of the limited duration of the ultrasonic experiments. To determine the general characteristics and to estimate the amount of water release from the sample at disequilibrium conditions, a thermogravimetric analysis (weight loss on ignition) was carried out. For this, a sample was heated incrementally up to temperatures of 1000 °C and weighed at each temperature step. With increasing temperature the weight decreases successively, leading to a total weight loss of 0.7 wt% at 1000 °C (Fig. 4.4), which is assumed to be related to the amount of water expelled during heating.
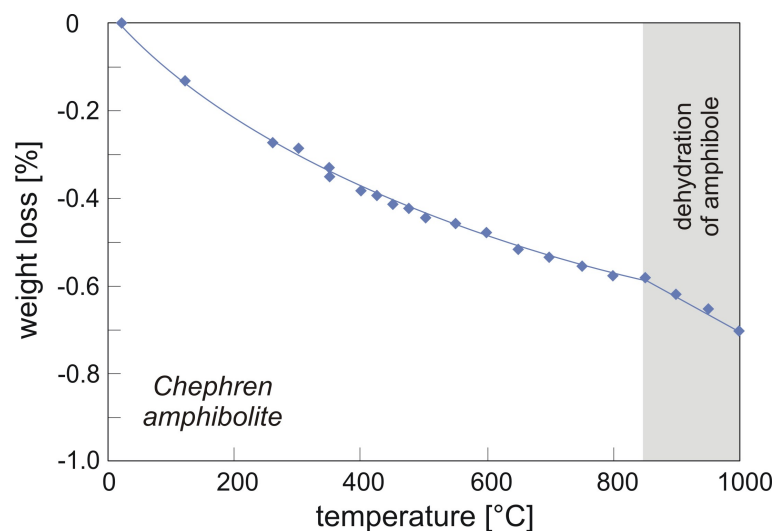

Figure 4.4: *Weight loss on ignition of the Chephren amphibolite at ambient pressure. The weight loss is attributed to water expelled from the sample. The weight loss is characterised by an exponential decrease at temperatures below 300 °C and almost linear relations at higher temperatures. In the low temperature range, the steeper part of the function is interpreted as the release of water in the pore space and adsorbed to the sample surface, while the linear part up to 850 °C might reflect a successive decomposition of water-bearing accessories (mica, pumpellyite, chlorite, epidote). The amphibole decomposition is related to the steeper decrease above 850 °C.*

The release of 0.7 wt% water is remarkably low, especially for an amphibolite, and suggests a water-undersaturation of the amphibole. This was verified using infrared spectroscopy (Fig. 4.5 and Appendix A.4), by which a mean water concentration of 0.35 wt% H_2O was found in the hornblende. For the amphiboles quenched at 800 °C and 800 MPa a slightly reduced mean water concentration of 0.29 wt% was derived (Fig. 4.5).

Moreover, IR-spectroscopy revealed that fresh amphiboles are extremely hygroscopic, bonding humidity from air. Thus, the single crystal spectra of the fresh sample do not only show the peaks of structurally bonded water ($3580 - 3740 \ cm^{-1}$), but also a broad reflex between $3100 - 3580 \ cm^{-1}$, which is related to molecular adsorbed water. The thermogravimetric analysis implies that about 0.3 wt% water is adsorbed to mineral surfaces of the starting material causing the slightly steeper decrease in the mass loss–temperature relation at temperatures lower than 300 °C.
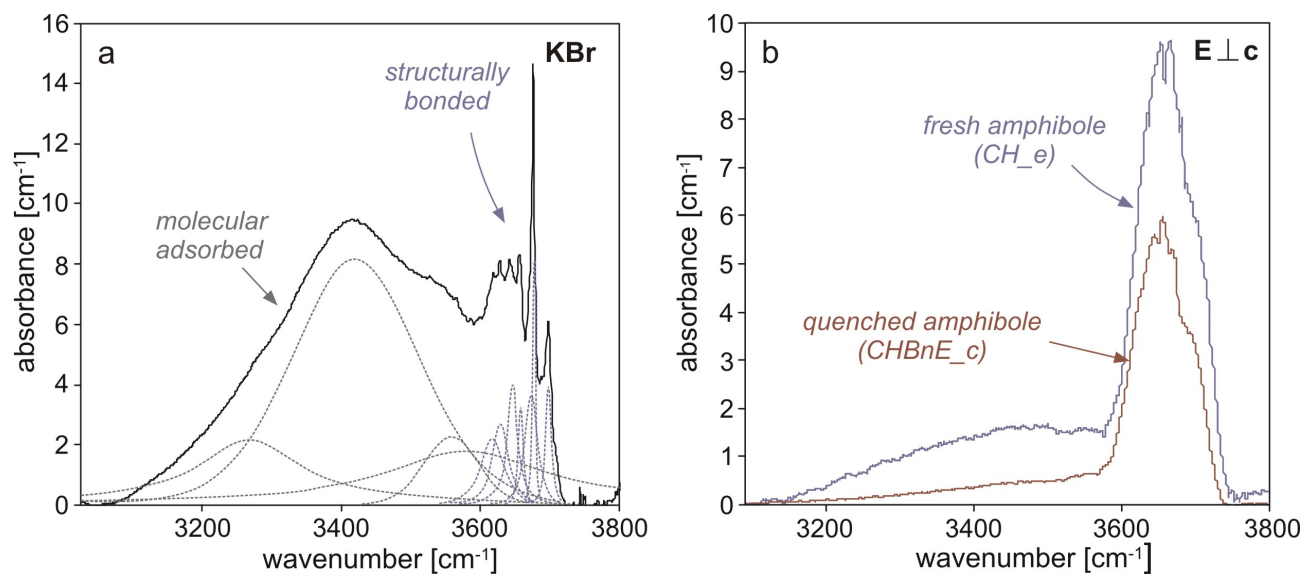
Figure 4.5: *Infrared amphibole spectra from Chephren amphibolite. Spectrum (a) was recorded on a KBr-tablet of the pre-run material. Dotted lines show the fitted peaks of structurally bonded water (blue) and molecular adsorbed water (grey). The integrated area of all peaks between 3600 and 3700 cm^{-1} is proportional to the H_2O concentration of the amphibole (Appendix A.4). (b) Single crystal spectra measured perpendicular to the c-axis. Black: a sample from the pre-run material. Red: a sample from an amphibolite quenched at 870 MPa and 800 °C. In quenched samples the affinity of water adsorption is clearly reduced.*

4.1.2   Texture and Structure

Pore Geometry and Grain Boundaries

Besides the mineral composition, the texture and especially the microstructure of a rock have a strong effect on its elastic wave velocity and are therefore described here. The Chephren amphibolite is characterised by a granoblastic, polygonal texture of medium grained plagioclase and amphibole minerals. The amphiboles are aligned and define the foliation of this rock. The grain size generally varies between 0.5 to 2 mm, but few smaller amphiboles with a size of about 0.2 mm were observed, too. The grain boundaries are predominantely straight, and triple junctions are developed with angles around 120 °, both indicating a textural equilibrium (Fig. 4.6a).

The open porosity was determined on the starting material (*pre-run samples*) as well as on samples quenched after ultrasonic experiments by means of the Archimedean Principle. Details of these measurements are decribed in Appendix A.2. The results are listed in Tab. 4.1. For the *pre-run samples* an open porosity of less than 0.15 % (±0.05) was determined, while after quenching subsequent to the experiment, a trend of increasing porosity with increasing experimental temperature is indicated. The geometry of pore space was investigated on thin-sections imbued with a fluorescent resin, analysed with a polarisation microscope in reflected UV light. This method allows to distinguish luminous voids from the black rock matrix.
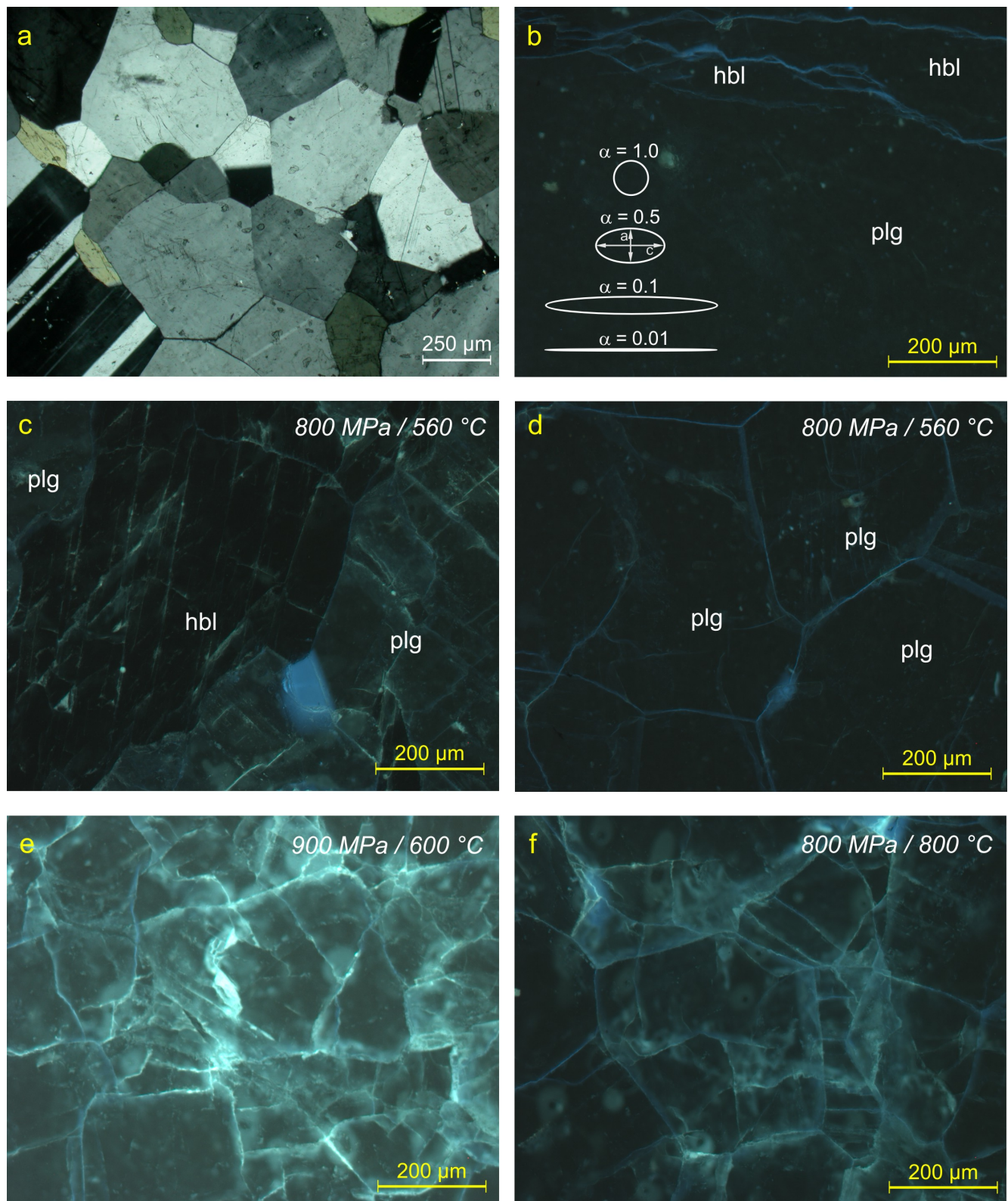
Figure 4.6: *a) Thin-section of Chephren amphibolite (crossed Nicols). Note the straight grain bounderies. Micrographs (b) to (f) were taken from thin-sections imbued with fluorescent resin and photographed under UV light. Cracks and pores can be identified by blue colours. (b) The pre-run sample shows almost no open porosity. (c to f) Micrographs of quenched samples. Obviously the porosity is defined by dilatant grain boundaries (plg) and cleavage planes (hbl) and possess a low aspect ratio $\alpha=(c/a)$. No round pores could be identified.*

Figure 4.7: *Micrographs of quenched Chephren amphibolite, with parallel nicols (a and c) and under reflected UV light (b and d). Micrographs (c) and (d) represent different areas in the same thin-section. Arrows in (d) point to echelon fractures.*
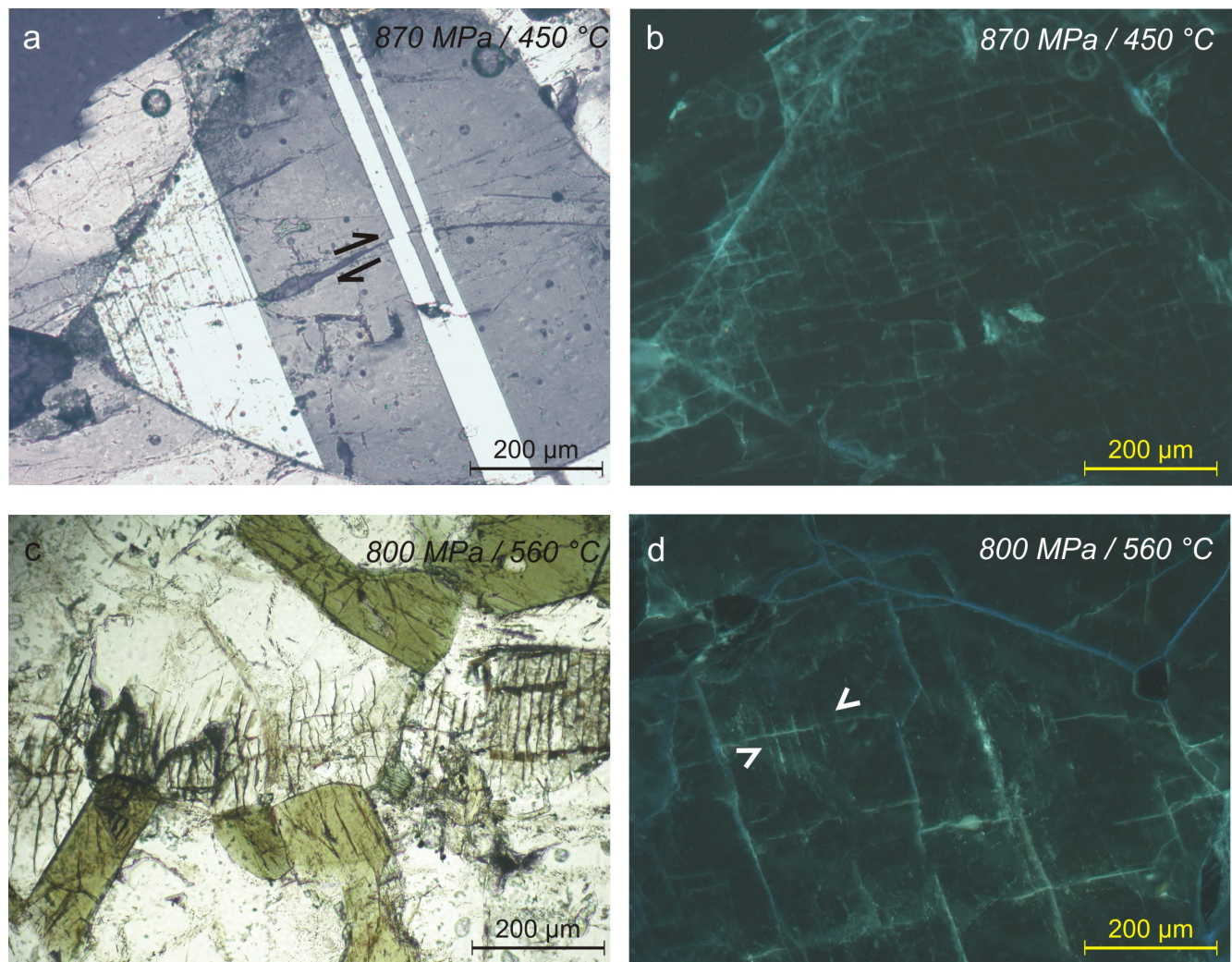
 Although sporadically grain boundaries and traces of cracks can be well identified in thin-sections from the *pre-run samples* (Fig. 4.1), the rock seems to be almost completely dense and exhibits only rare open cracks with irregular surfaces (Fig. 4.6). The cracks are oriented within the foliation plane, transecting amphibole aggregates and plagioclases. No evidence for weak grain contacts is observed.

In contrast, *quenched samples* possess fairly well developed fracture frameworks which are linked primarily to the grain boundaries and follow the cleavage planes of the minerals (Figs. 4.6c and d). With increasing temperature, cracks seem to dilate locally and form a dense network of fractures (Figs. 4.6e and f). Especially plagioclase seems to be subjected to brittle deformation, exhibiting internal deformation structures. Fig. 4.7 a and b show a plagioclase grain quenched at 900 MPa and 450 °C, which was located at the margin of the sample. The twin planes are slightly displaced and under UV light an intense fracturing of the whole grain is obvious. In another sample (Fig. 4.7 c and d), quenched at 800 MPa

sample	exp. conditions		open porosity [%]	
number	T_q [°C]	P_c [MPa]	before exp.	after exp.
CHA	446	870	0.237	1.587
CHD$_2$	500	750	0.102	1.191
CHE$_2$	500	800	0.012	1.220
CHC$_2$	500	850	0.009	1.123
CH$_{21c}$	540	800	0.106	1.203
CHC$_1$	560	800	0.047	1.344
CHD$_1$	600	900	0.029	1.390
CH$_{21b}$	660	900	0.095	1.438
CHE$_1$	700	800	—	1.344
CHB	800	800	0.152	1.427
Ma20	750	900	0.178	1.677
T_q = quenching temperature, P_c = confining pressure				

Table 4.1: *Comparison of sample porosities of the Chephren amphibolite (**CH**) and Malenco serpentinite (**Ma**) before and after the experiments. The quenching at high P_c took < 2 min, the pressure release 10 h and more to reduce a post-experimental porosity increase.*

and 560 °C, bands of cataclastic microfractures were observed. These bands are defined by a number of small, nearly parallel aligned cracks, which run through plagioclase grains. The fracture bands can be identified with UV light (note arrows in Fig. 4.7 d), pointing to a certain porosity in these structures. Before and after the ultrasonic experiments the pore volume is restricted to cracks and loose grain contacts. No round pores could be identified. As a consequence the pore geometry is predominantly defined by voids with small aspect ratios, whereby the aspect ratio α is defined as the ratio of shortest to longest axis of a rotational ellipsoid (Fig. 4.6 b). Fracture bands and open grain boundaries were not observed in the *pre-run samples*. Hence, the internal deformation of the sample is assumed to be caused by the *PT*-treatment during the experiment or by quenching of the sample after the experiment rather than to represent relicts of the sample history.

The Lattice Orientation

The Chephren amphibolite allows a detailed analysis of the crystallographic orientation of the main rock-forming minerals, as it has a medium grain size and simple mineralogical composition. The quantitative analysis was performed by **e**lectron **b**ack-**s**catter **d**iffraction (EBSD) technique at the Laboratoire de Tectonophysique at Université Montpellier II, France. Details of the method are described in Appendix A.5. The lattice preferred orientations (LPO's) were determined on thin-sections cut parallel to the foliation plane (XY-plane). For an easier comparison with literature data the LPO's were subsequently rotated and are presented as equal area, lower hemisphere stereographic projections in the structural XZ-reference frame (Fig. 4.8). In this projection Z represents the pole of foliation, which in turn runs vertically in E-W direction related to the structural frame. The lineation, X, is oriented horizontally and Y
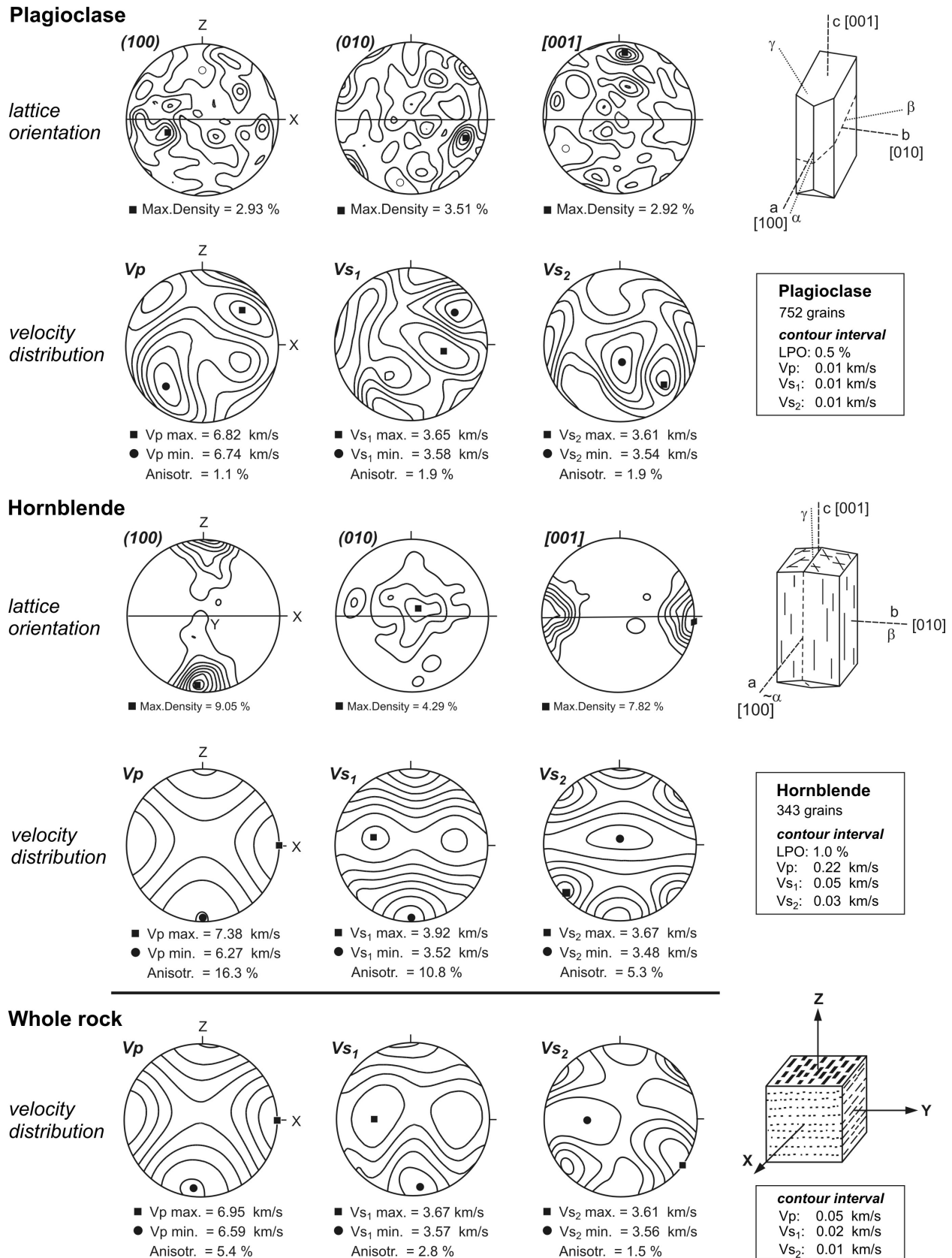
Plagioclase

lattice orientation

(100) Max.Density = 2.93 %

(010) Max.Density = 3.51 %

[001] Max.Density = 2.92 %

velocity distribution

Vp
- Vp max. = 6.82 km/s
- Vp min. = 6.74 km/s
- Anisotr. = 1.1 %

Vs₁
- Vs₁ max. = 3.65 km/s
- Vs₁ min. = 3.58 km/s
- Anisotr. = 1.9 %

Vs₂
- Vs₂ max. = 3.61 km/s
- Vs₂ min. = 3.54 km/s
- Anisotr. = 1.9 %

Plagioclase
752 grains
contour interval
LPO: 0.5 %
Vp: 0.01 km/s
Vs₁: 0.01 km/s
Vs₂: 0.01 km/s

Hornblende

lattice orientation

(100) Max.Density = 9.05 %

(010) Max.Density = 4.29 %

[001] Max.Density = 7.82 %

velocity distribution

Vp
- Vp max. = 7.38 km/s
- Vp min. = 6.27 km/s
- Anisotr. = 16.3 %

Vs₁
- Vs₁ max. = 3.92 km/s
- Vs₁ min. = 3.52 km/s
- Anisotr. = 10.8 %

Vs₂
- Vs₂ max. = 3.67 km/s
- Vs₂ min. = 3.48 km/s
- Anisotr. = 5.3 %

Hornblende
343 grains
contour interval
LPO: 1.0 %
Vp: 0.22 km/s
Vs₁: 0.05 km/s
Vs₂: 0.03 km/s

Whole rock

velocity distribution

Vp
- Vp max. = 6.95 km/s
- Vp min. = 6.59 km/s
- Anisotr. = 5.4 %

Vs₁
- Vs₁ max. = 3.67 km/s
- Vs₁ min. = 3.57 km/s
- Anisotr. = 2.8 %

Vs₂
- Vs₂ max. = 3.61 km/s
- Vs₂ min. = 3.56 km/s
- Anisotr. = 1.5 %

contour interval
Vp: 0.05 km/s
Vs₁: 0.02 km/s
Vs₂: 0.01 km/s

Figure 4.8: *Pole-figures of hornblende and plagioclase orientation with respect to the XZ-plane (perpendicular to foliation and lineation) of Chephren amphibolite. For both LPO's the velocity distribution is calculated. The bottom line shows the calculation of the velocity distribution in the Chephren amphibolite on the basis of 64 % plagioclase and 36 % hornblende. The calculations of single crystal velocities as well as the whole rock velocity are based on Voigt-Reuss-Hill averaging.*

marks the structural axis normal to the lineation within the foliation plane. Because of the relative large grain size of the amphibolite, the thin-sections were measured grain by grain. Altogether the LPO's of the two major constituent mineral phases plagioclase and hornblende were identified. Their pole-figures are shown in Fig. 4.8. The plagioclase grains appear to be almost randomly oriented. In contrast, amphibole crystals have a lattice preferred orientation, which is defined by a significant concentration of (100)-poles normal to the foliation (in Z-direction) and [001]-axes parallel to the lineation (X-direction). (010)-poles possess typically a maximum density close to the Y-axis.

The velocity of wave propagation in a polycrystalline material depends on the single crystal velocities, the volume fraction of the constituent minerals, and textural particularities. The three-dimensional distribution of seismic velocities of an idealised pore-free Chephren amphibolite were calculated from its major rock-constituting minerals regarding single crystal densities (plagioclase: 2.6 g/cm^3; hornblende: 2.9 g/cm^3), elastic stiffness coefficients [Aleksandrov et al., 1974; Aleksandrov & Ryzhova, 1961], LPO's and the volume fraction of plagioclase and hornblende. The procedure was performed with a program developed by Mainprice [1990] by use of the Christoffel equation. The averaging scheme for elastic constants is based on a Voigt-Reuss-Hill averaging scheme [Hill, 1952]. Details of the calculation are discussed e.g. in Crosson & Lin [1971], Baker & Carter [1972], and Peselnick et al. [1974]. Additionally, the velocities of plagioclase and hornblende were calculated in terms of their orientation in the rock. As plagioclase is randomly oriented, the pronounced alignment of the highly anisotropic hornblende defines the velocity anisotropy (Fig. 4.8).

The calculated velocities refer to ambient conditions (room *PT*). No pressure- and temperature dependent elastic constants are available for the low-symmetry minerals plagioclase and hornblende, yet. Thus, no theoretical development of the velocities as a function of pressure and temperature was modelled.

4.2   Malenco Serpentinite

4.2.1   Mineral Assemblage

The *Malenco serpentinite* is composed of 39.1 vol% antigorite, 42.9 vol% forsterite, 12.6 vol% diopside, 3.1 vol% hedenbergit, 1.4 vol% chlorite, and accessories (Fig. 4.9a and b). It is thus, strictly speaking, a serpentinised peridotite and is assumed to represent tectonically denuded oceanic or subcontinental mantle [Froitzheim & Manatschal, 1996; Manatschal & Nievergelt, 1997]. Nonetheless, for simplification it will be referred to here as "serpentinite". Olivine and clino-pyroxenes form separate domains in a micocrystalline to fibrous antigorite matrix. The ore phases magnetite, pentlandite, and ilmenite make together about 1 vol% and represent the minor mineral phases in the *Malenco serpentinite*.
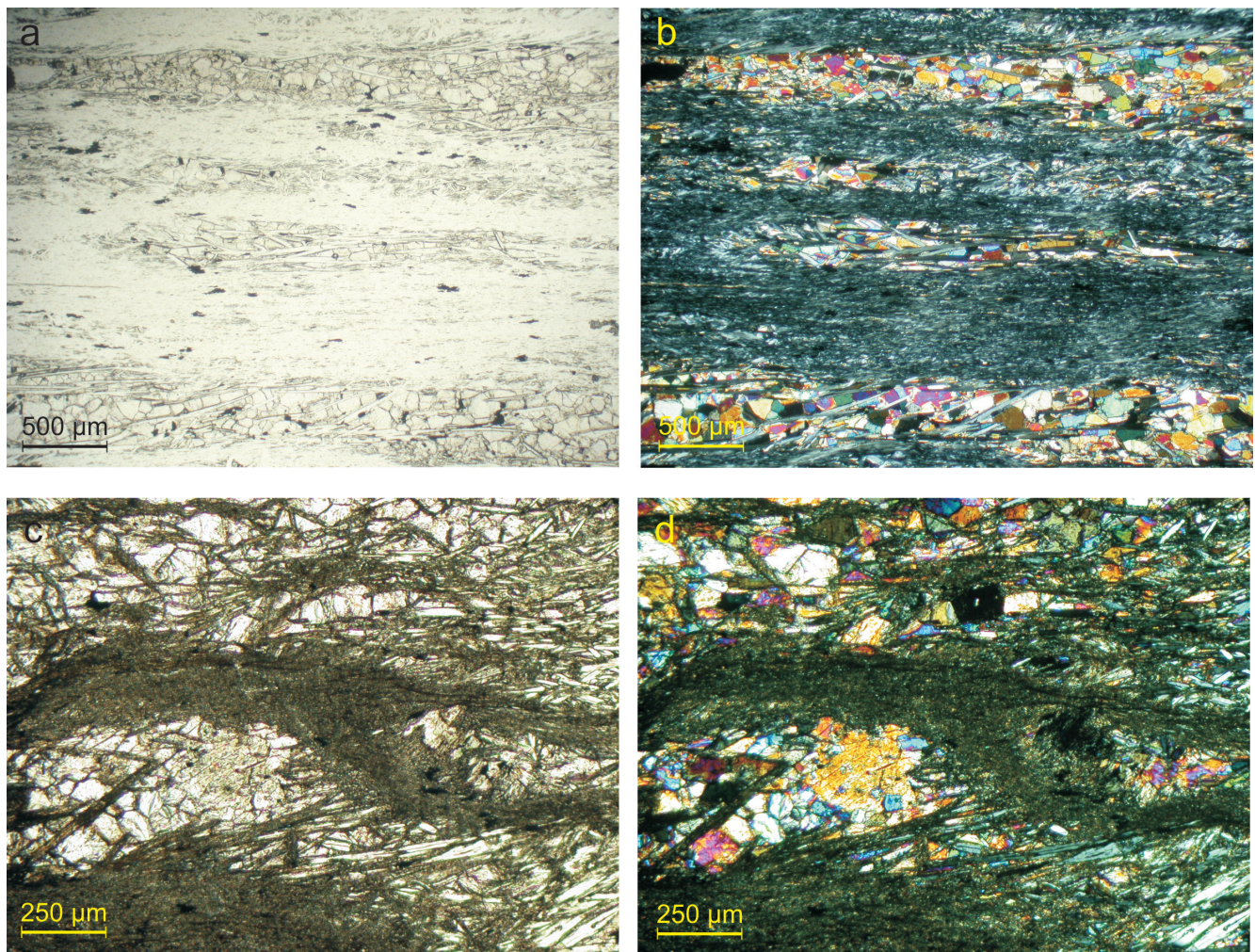

Figure 4.9: *Thin-sections of Malenco serpentinite recorded with parallel and crossed polarisers. (a and b) were taken from the starting material and (c to d) from the sample, quenched at 900 MPa and 750 °C.*
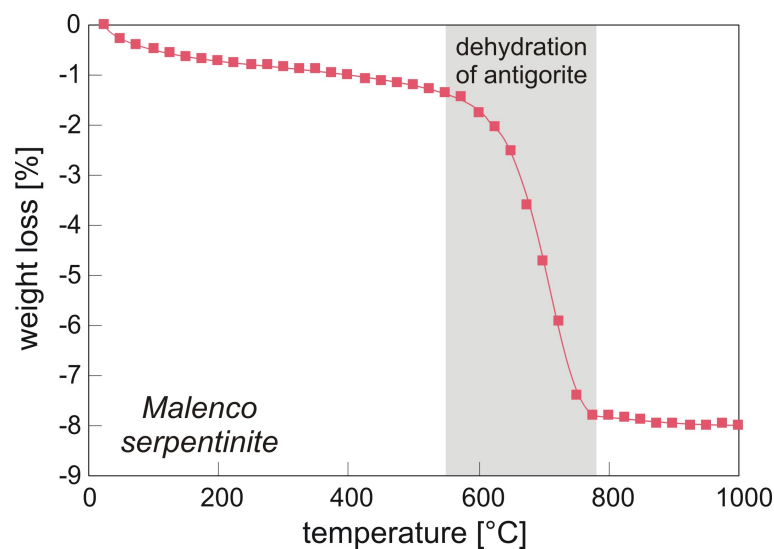
Figure 4.10: *Weight loss on ignition of the Malenco serpentinite with temperature at ambient pressure, which is attributed to the release of water. The Malenco serpentinite is characterised by a discontinuous water release. The decomposition of antigorite can be related to the steep decrease in mass between 600 and 750 °C.*

The sample, quenched after the ultrasonic experiment at 900 MPa and 750 °C, shows locally a decomposition of antigorite to talc. Additionally, areas near cracks are characterised by a fine distribution of a microcrystalline, opaque mineral phase, which seems to be a nickel oxid.

Compared to the Chephren amphibolite, the serpentinite is characterised by a discontinous water release at ambient pressure. Till the onset of heating, a decrease in weight of about 1.25 % was observed. This may be predominantly related to water adsorbed to the sample surface (Fig. 4.10). The dehydration of serpentine occurs in a relatively narrow temperature interval between 600 and 750 °C and is defined by a total weight loss on ignition of about 7 %.

4.2.2   Texture and Structure

The Malenco serpentinite is characterised by a density of 2.88 g/cm^3 and an open porosity of less than 0.2 vol-% ($\pm$0.01), which increase to 1.7 % in the quenched sample (Tab. 4.1).

Similar to the amphibolite, the serpentinite is foliated. The foliation is defined by lenticular areas of granular peridotitic material, such as olivine, and pyroxene, which are embedded in antigorite layers. At the margins of peridotitic lenses the antigorite fibres form bunch-like aggregates. Generally, the serpentinite shows a grain size of less than 0.25 mm, but some antigorite fibers exhibit longest axes of up to 0.5 mm. In general, the microstructure of the serpentinite gives the impression of interlocked grain boundaries (Fig. 4.11a).
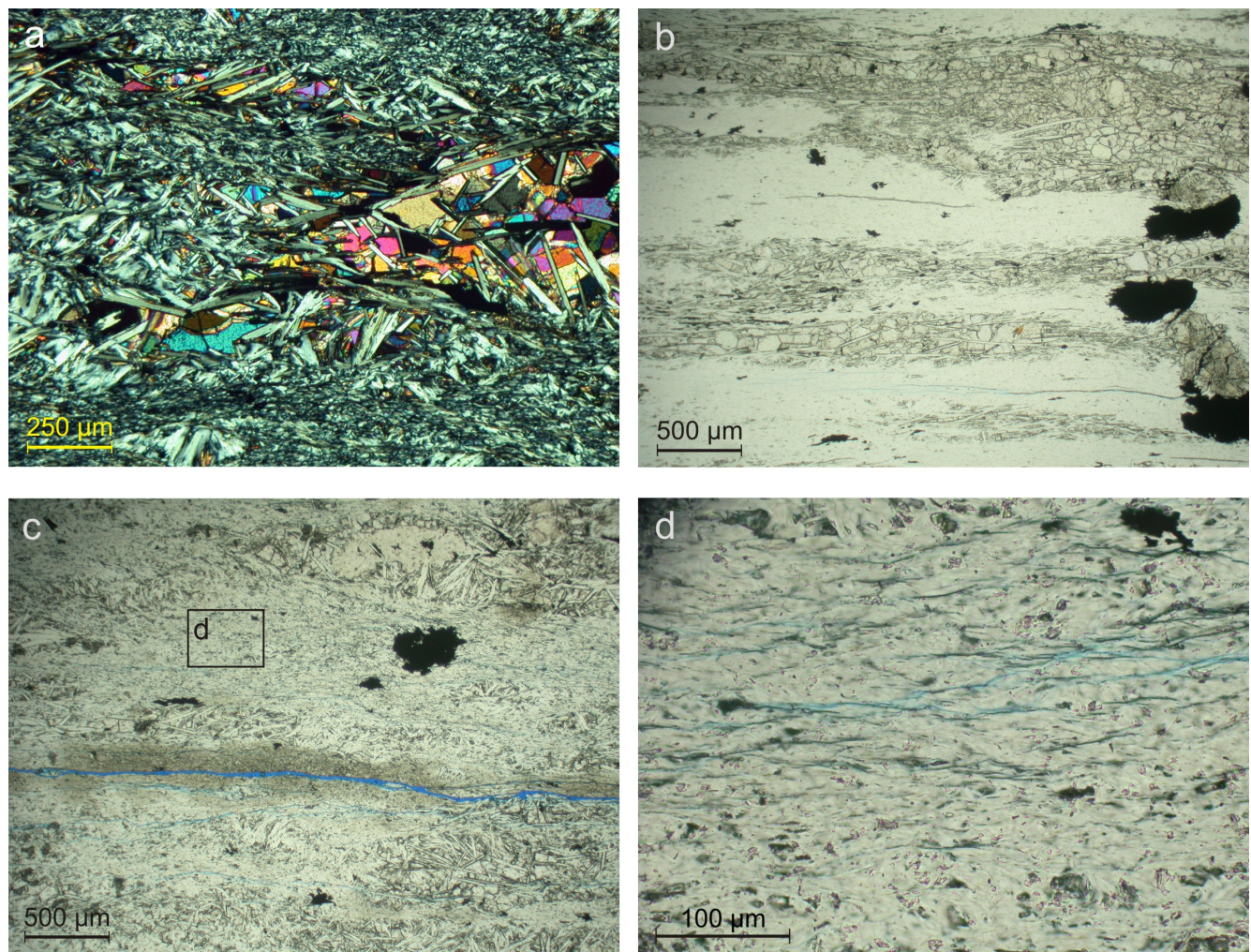
Figure 4.11: *Details of the microstructure of the Malenco serpentinite. (a) The antigorite needles form interlocked mineral aggregates. Micrographs (b to d) were taken from thin-sections stained with a blue epoxy resin. (b) Note that the pre-run sample shows almost no porosity. Only a thin crack is obvious in the lower part of the micrograph. (c) A considerably higher porosity was observed in the quenched sample. The marked area is enlarged in (d) and indicates the formation of a fine estuary of cracks.*

Fig. 4.11 shows micrographs of the original Malenco serpentinite *pre-run sample* and the *quenched sample*, both stained with a blue epoxi resin to make pores visible (Figs. 4.11 b to d). Again, as in case of the *Chephren amphibolite*, the porosity of *Malenco serpentinite* is defined by voids of a small aspect ratio. In the *pre-run sample* only few, fine cracks of a length of 1 - 1.5 mm were observed in the antigorite matrix. In the *quenched sample*, cracks dilated considerably and show lengths in cm-scale. Locally, larger areas of antigorite matrix are crisscrossed by a fine estuary of cracks, preferrently oriented in the foliation plane.